



The Roles of Threading Dislocations on Electrical Properties of AlGaIn/GaN Heterostructure Grown by MBE

Yuen-Yee Wong,^a Edward Yi Chang,^{a,b,z} Tsung-Hsi Yang,^{b,c} Jet-Rung Chang,^b Jui-Tai Ku,^d Mantu K. Hudait,^e Wu-Ching Chou,^d Micheal Chen,^f and Kung-Liang Lin^a

^aDepartment of Materials Science and Engineering, ^bDepartment of Electronics Engineering, ^cMicroelectronics and Information System Research Center, and ^dDepartment of Electrophysics, National Chiao Tung University, Hsinchu 30010, Taiwan

^eDepartment of Electrical and Computer Engineering, Virginia Tech, Blacksburg, Virginia 24061, USA

^fULVAC Taiwan Incorporated, Hsinchu 30078, Taiwan

The role played by different types of threading dislocations (TDs) on the electrical properties of AlGaIn/GaN heterostructure grown by plasma-assisted molecular beam epitaxy (MBE) was investigated. Samples with different defect structures and densities were prepared and measurements were taken from the same sample to study the correlative behavior of various TDs. From the Hall measurement, the electron mobility in two-dimensional electron gas channel was mainly controlled by the edge dislocation, which has a dominant amount in the material. The edge TDs acted as Coulomb scattering centers inside the channel and reduces the carrier mobility and increased its resistance. Screw TDs played a much significant role than edge TDs in determining the reverse-bias leakage current of Schottky barrier diodes. Leakage current is affected slightly by the reduction of free carrier density in the channel for samples with a higher edge TD density, but screw TD, which acted as the current leakage path, was more deleterious to the reverse-bias leakage current of AlGaIn/GaN structure.

© 2010 The Electrochemical Society. [DOI: 10.1149/1.3392365] All rights reserved.

Manuscript submitted January 19, 2010; revised manuscript received March 9, 2010. Published May 17, 2010.

GaN high electron mobility transistor (HEMT) devices are excellent candidates for high power and high frequency applications.^{1,2} GaN HEMTs are usually achieved by using either AlGaIn or AlInN as the barrier layer on top of a GaN buffer layer. Due to the strong polarization effect and large amount of surface states, high electron density can be induced at the AlGaIn/GaN or AlInN/GaN interfaces, as two-dimensional electron gas (2DEG) without any intentional doping in the materials.^{3,4} However, GaN and its heterostructure materials are usually epitaxial grown on a foreign substrate, such as sapphire, silicon, or silicon carbide because a large-size commercial grade native substrate is still not available at a low cost. A high density of threading dislocation (TD) is therefore generated in the materials as a result of large lattice and thermal expansion coefficient mismatches between the GaN films and these substrates. TDs are known to induce electron scattering in the GaN material, thus reducing the carrier mobility,⁵⁻⁷ and increasing the current leakage path in GaN-based devices.^{8,9} High electron mobility in the 2DEG and low reverse-bias leakage current at the gate are the two most important parameters for GaN-based HEMTs to achieve a high power performance at high frequency operations. In a lateral current flow electron device, the former is controlled by factors affecting electron moving transversely in the channel, while the later is determined by factors influencing current flow vertically across the barrier material. Three types of TDs are normally associated with the hexagonal material of GaN, namely, screw type, edge type, and mixed type. It is believed that each of the TD types may play different roles in the GaN HEMT. However, most of the previous results on the dislocation in GaN materials were obtained on the GaN film,^{5,10,11} but did not consider the HEMT devices, while others were measuring the performance of GaN HEMT as a function of the total dislocation density,⁶⁻⁸ but did not take into account the role played by each type of dislocation. In fact, the structural and electrical properties of dislocation are not only depended sensitively on the dislocation type but also on the growth method, growth conditions as well as the presence of dopants and impurities. For example, theoretical calculation have shown that both the screw and edge TDs are electrically inactive with a bandgap free from deep levels in the absence of impurities.¹² However, the characterizations on real samples revealed that most of the TDs in GaN are in fact electrically active. The dislocation core can be filled up with excess Ga

atoms^{11,13} or dopants and impurities (including Mg, Si, and O),¹³ and therefore, changing the core structure and creating extra energy states in the material bandgap. In this paper, we have investigated the effect of screw and edge TDs on the electrical properties, namely, the electron mobility and reverse-bias leakage current of AlGaIn/GaN heterostructure grown by plasma-assisted molecular beam epitaxy (PAMBE). Both carrier mobility and reverse-bias leakage current were obtained from the same sample and therefore their correlative behavior can be studied.

Experimental

The AlGaIn/GaN heterostructures were grown by PAMBE [ULVAC Molecular Beam Epitaxy (MBE) System] on sapphire (0001) substrates. The epi-ready substrates were first thermally cleaned in the growth chamber at 820°C until the reflection high energy electron deflection (RHEED) pattern became streaky. Nitridation of the substrate was then performed at 600°C to form a starting layer for the deposition of AlN buffer and followed by 1.5 μm GaN film. In this study, a series of AlGaIn/GaN heterostructures with different amounts of screw and edge TDs were achieved by modifying the growth condition of AlN and the initial growth condition of GaN layers. In all cases, the final surfaces of GaN layers were smooth as indicated by the streaky RHEED patterns. Finally, AlGaIn layers with constant Al composition of 25% with two different thicknesses (20 and 25 nm) were grown on the GaN layers. Atomic force microscope (AFM, Digital Instrument, D3100) was used to investigate the as-grown sample surfaces. Defect structure of the AlGaIn/GaN heterostructures was determined by high resolution X-ray diffractometry (HRXRD, Bede D1 system) scanning on the rocking curves of different diffraction planes. The aluminum composition and thickness of each AlGaIn barrier layers were also determined by HRXRD, using ω-2θ and X-ray reflectivity scan modes, respectively. After the structural characterization, each of the samples was divided into two parts and prepared for Hall measurement and Schottky barrier diodes (SBDs) fabrication. From the Hall measurement using the van der Pauw contact configuration, electron mobility, sheet resistance, and carrier density of 2DEG were obtained. SBDs fabricated on the AlGaIn/GaN samples were used to measure the reverse-bias current. Before the fabrication, any metal droplet on the wafer surfaces was removed using diluted hydrochloric acid. The circular SBDs consist of a Schottky contact with diameter of 130 μm at the center of diode, and an ohmic contact formed as the outer ring. Using standard photolithography and lift-off methods, the

^z E-mail: edc@mail.nctu.edu.tw

Table I. fwhm of GaN(0002) and (10–12) planes prepared on buffers with different growth conditions.

Sample	AlN buffer growth temperature (°C)	fwhm of rocking curve (arc sec)		AlGaIn thickness (nm)
		(0002) plane	(10–12) plane	
A	740	71	2404	20
B	700	85	2276	20
C	550	264	1890	20
D	800	75	2584	20
M	800	100	1460	25
N	750	233	1221	25

ohmic contacts of SBD were first fabricated by depositing Ti (200 Å)/Al (1200 Å)/Ni (250 Å)/Au (1000 Å) and followed by rapid thermal annealing at 800°C for 1 min. Then, the Schottky contact was formed by depositing Ni (200 Å)/Au (3000 Å).

Results and Discussion

In a previous study,¹⁴ we have shown that the defect structure of GaN can be controlled by the growth condition of AlN buffer layer. Generally, if the starting surface of the AlN layer was relatively rough, the edge TDs in GaN were grown in the inclined direction and their self-interaction was enhanced. Therefore, the amount of edge TD density could be reduced through the recombination and annihilation processes. The formation of screw TD in GaN was suppressed on a smooth buffer surface. In this work, samples A, B, C, and D were prepared by using different AlN growth temperatures with constant thickness of 15 nm. By changing the growth temperature of AlN buffer from 550 to 800°C, GaN layers with different dislocation densities, as indicated by the full width at half-maximum (fwhm) values of the rocking curves, were prepared as shown in Table I. To further reduce the edge TD density, a second buffer layer of GaN grown under Ga-lean condition was also deposited on the AlN for samples M and N. The GaN materials grown under this condition would have surface with inclined facets which could further enhance the bending of edge TD propagation direction and reduce its density.^{15,16} On top of all these buffers, initial GaN layer grown under Ga-rich growth condition was first applied to recover the rough surface of these buffer layers. Once the GaN surface became smooth (within tens of nanometers), as indicated by the streaky RHEED patterns, the effective Ga/N ratio was set to slightly larger than unity for the rest of the growth to ensure a smooth surface of GaN layer was maintained. AFM images show the typical surface morphologies of GaN (Fig. 1a) and AlGaIn (Fig. 1b) grown in this study. The surface of AlGaIn decorated by small “mounds” is believed to be the result of kinetic roughening in the MBE growth of the AlGaIn material.¹⁷ The root-mean-square roughnesses were 0.44 and 0.65 nm, respectively, on a 4 μm² area. The RHEED patterns of these surfaces are also shown in the insert of each diagram.

The dislocation densities of the GaN samples were determined using HRXRD. X-ray rocking curves (ω-scan) of both symmetric (0002) and asymmetric (10–12) planes were scanned for these samples. Due to the specific defect structure of screw TD (with Burgers vector $b = \langle 0001 \rangle$), edge TD ($b = 1/3 \langle 11-20 \rangle$), and mixed TD ($b = 1/3 \langle 11-23 \rangle$), the (0002) rocking curve is broadened by screw- and mixed-type TDs, while the (10–12) rocking curve is broadened by all TDs.^{18,19} The contribution of both screw and edge TDs to the rocking width can be distinguished using the following equation

$$\beta_{(10-12)}^2 = \beta_s^2 + \beta_e^2 \quad [1]$$

where $\beta_{(10-12)}$ is the fwhm of (10–12) plane and β_s and β_e are the contributions of screw and edge TDs, respectively, to the fwhm of (10–12) plane.¹⁸ To simplify the calculation of the dislocation densities, the mixed TDs have been divided into their screw- and edge-

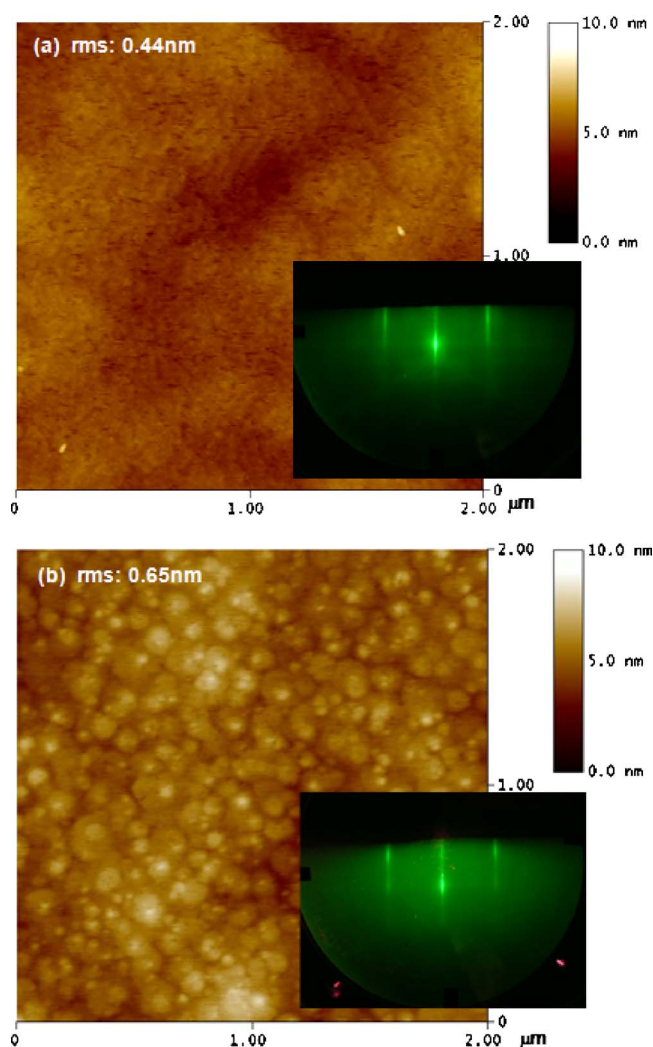


Figure 1. (Color online) AFM images of the typical as-grown (a) GaN and (b) AlGaIn surfaces. Inserts show their corresponding RHEED patterns.

type components. So the “screw TD” in this study is referred to the contribution from pure screw and the screw component of mixed TDs, while the “edge TD” is consisted of pure edge and the edge component of mixed TDs. Furthermore, it was also demonstrated by Gay et al.²⁰ that the dislocation density is related to the XRD result through the equation

$$D_{\text{dis}} \sim \beta^2/9b^2 \quad [2]$$

where D_{dis} is the TD density in the material, β is the fwhm of a given XRD peak, and b is the length of Burgers vector of their corresponding dislocation. From Eq. 1 and 2, both the screw and edge TD densities in GaN can be calculated.¹⁴

The effects of dislocation in the GaN film were compared with the electron mobility obtained from the Hall measurements. Figure 2 shows the relationship between the electron mobility and edge TD density in the AlGaIn/GaN samples. The mobility is decreased monotonically with the increase in the edge TD density in the samples. For sample D, with an edge TD density of more than 1.7×10^{10} cm⁻², the mobility cannot be measured due to the over-ranged sheet resistance ($>10^6$ ohm/square) and has been set as zero. The reduction in the electron mobility in the AlGaIn/GaN samples can be explained by considering the edge-type TD as the scattering centers for electrons moving in the 2DEG. The dangling bonds along the edge dislocation line can act as an electron acceptor^{5,6} and filled up with electrons from the channel. Therefore,

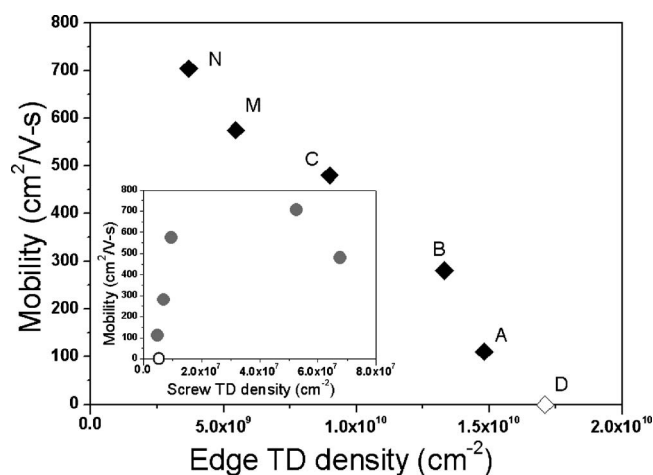


Figure 2. Hall electron mobility of AlGaIn/GaN samples as a function of edge TD density. Insert shows the effect of screw TD density on electron mobility. Open symbols in the diagrams represent the values for sample D.

these negatively charged edge dislocations scattered and reduced the carrier mobility. This is supported by the reduction of sheet carrier density with the increase in the edge TD density as shown in Fig. 3. All the AlGaIn layers were grown under the same growth condition (despite two different thicknesses, these thicknesses are well above the critical thickness (~ 35 Å) required to induce carriers into 2DEG³ from the surface state) and the carrier concentrations induced in the 2DEG are supposed to be similar for all the samples. It is the occurrence of trap sites in the dislocations that has reduced the availability of electron as free carriers in the 2DEG. As a result, the measured sheet resistances also increase accordingly. For a better illustration of the effect of the edge TD, the sheet resistance and free carrier concentration for sample D are set as 10^6 Ω/□ and zero, respectively.

In AlGaIn/GaN structure, electrons are confined in the 2DEG formed at the close vicinity of the heterostructure interface. These carriers are moving parallel to the AlGaIn/GaN interface and therefore their mobility can be affected by a variety of factors, such as phonon scattering, interface roughness, alloy scattering from the Al-GaN barrier, and scattering from the charged defects (dislocations, dipoles, residual impurities).²¹ Because the growth condition of AlGaIn/GaN is similar for all the samples in our experiment, these

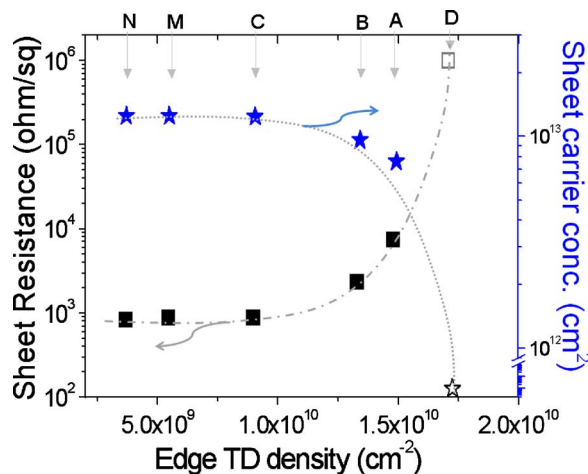


Figure 3. (Color online) Sheet resistance and carrier concentration of the AlGaIn/GaN samples as a function of edge TD density. Open symbols represent the values for sample D.

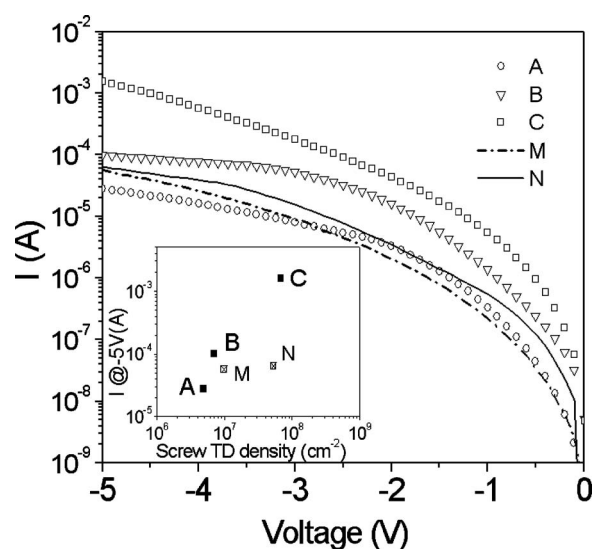


Figure 4. The reverse bias currents of AlGaIn/GaN SBD samples. Insert shows the reverse bias current for samples A, B, and C at -5 V as a function of screw TD density.

factors are the invariance properties except the TD density. The electron mobility decreases proportionally with the increase in the edge TD density, at least in the density range in this study.

There is no clear relationship between the electron mobility and screw TD density (insert of Fig. 2). This is understandable because the edge TD densities in all the samples are at least 2 orders of magnitude larger than the screw TD densities. For GaN materials grown on sapphire by common methods such as MBE and metalorganic chemical vapor deposition, the dislocation is always dominated by edge TD. The effect of the screw dislocation on electron mobility could have been overshadowed by the presence of the large number of edge dislocations. However, it is still reasonable to suggest that the screw TD does not play a significant role in controlling the electron mobility in most of the common cases.

Another important parameter of HEMT device is the reverse-bias leakage current at the gate contact. This current can be originated from both the surface and bulk material of the AlGaIn/GaN structure. In this work, only factors controlling the bulk component are investigated and the surface leakage currents are assumed similar for all the samples because they were grown under the same condition. Bulk leakage mechanism play the dominant role in the reverse-bias current²² and it is believed that the TD is the major factors controlling this property, as suggested by the literatures.^{9,23} The leakage currents of the AlGaIn/GaN structures were determined from the fabricated SBDs. For useful comparison, only samples A, B, C, M, and N, with measurable sheet resistances and current densities, have been fabricated into SBDs. Leakage current in SBDs is flowed vertically across the AlGaIn layer as in contrast to the Hall measurement with electrons moving transversely in the 2DEG. The quality of AlGaIn layer is, therefore, crucial under this circumstance. In the present study, crystal qualities of the AlGaIn layers are too thin to be determined using HRXRD. Because they were all grown continuously on GaN without applying a growth stop, the dislocations in AlGaIn are presumed to be similar to or imitate most of those from the GaN layers. The strain induced from the lattice mismatches between these two materials was believed only to bend TDs slightly in the growth direction, but did not obstruct dislocation from propagating to the sample surface. The leakage currents measured at reverse-bias for the AlGaIn/GaN samples are shown in Fig. 4. For samples A, B, and C, all with AlGaIn thickness of 20 nm, the amount of leakage current increases with increasing screw TD density. Insert of Fig. 4 shows the values of leakage current measured at the reverse-bias of 5 V for these samples. For MBE grown GaN materials, the

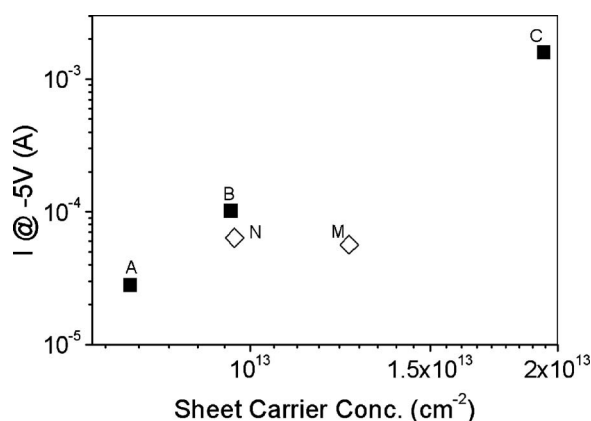


Figure 5. The reverse bias currents of AlGaIn/GaN SBD samples as a function of sheet carrier density in the 2DEG.

screw dislocations acted as a leakage path for reverse-bias current as suggested by Hsu et al.⁹ Their study also revealed that the screw dislocations, which are likely to be associated with excess Ga under Ga-rich growth condition, have a relaxed core and become electrically active.¹¹ For samples M and N, with AlGaIn thickness of 25 nm, their leakage also increased with screw TD density, but with a much slower rate. This has suggested that the longer leakage paths in the thicker AlGaIn layers have increased the resistance for the leakage current.

The influence of the edge TD density on the leakage currents is not following a clear trend. At first thought, the availability of the free carrier density in the 2DEG (decrease with edge TD density) seems to limit the amount of leakage current as shown in samples A, B, and C (with thinner AlGaIn layer). But it is not the case for samples M and N (with thicker AlGaIn layer). Although the edge TD densities are much higher than the screw TD densities, the role of the latter is dominant in this case. If only samples A, B, and C are compared, the slope of the insert of Fig. 4 is much steeper than the one in Fig. 5. This has suggested that the screw dislocation plays a more important role than the edge dislocation in affecting the reverse-bias leakage current of the AlGaIn/GaN structure.

Conclusion

In this study, the roles of TD on the electrical properties of AlGaIn/GaN structure have been investigated. These properties, namely, electron mobility in the 2DEG and reverse-bias leakage current at the gate contact, were determined from the Hall measurement and SBDs, respectively. GaN materials with different defect structures and densities, which have been estimated using HRXRD, were first achieved by controlling the growth conditions of both AlN and GaN buffer layers. As the dominant type of dislocation in GaN, the edge TD affects the electron mobility in the 2DEG. They tended to trap carriers in the channel and in turn, acted as the scattering center to reduce the electron mobility. As a result, the availability of the free carrier density was reduced, while the channel resistance was increased with the increase in the edge TD density. The screw TD seemed to not affect the electron mobility significantly, but

served as the major player in controlling the reverse-bias leakage current. Each of the screw TD may provide a conducting path in the AlGaIn layer for the leakage current and therefore a thicker barrier layer could be used to suppress the leakage current. This is because the current resistance was increased due to the longer leakage paths in the thicker AlGaIn layer. The availability of free carrier density in the 2DEG, which is a function of edge TD density, also seems to affect the leakage current for sample with thinner AlGaIn layer, but the effect is relatively insignificant as compared to the effect of the screw TD density.

Acknowledgment

This work was financially supported by the Ministry of Economic Affairs and the National Science Council of Taiwan under research grant no. 95-EC-17-A-05-S1-020, no. NSC95-2752-E-009-001-PAE, and no. NSC96-2221-E-009-236. The authors thank UL-VAC Taiwan Inc., Micheal Chen, and Stanley Wu for the MBE maintenance support.

National Chiao Tung University assisted in meeting the publication costs of this article.

References

1. N. Onojima, N. Hirose, T. Mimura, and T. Matsui, *Jpn. J. Appl. Phys.*, **48**, 094502 (2009).
2. A. Chini, R. Coffie, G. Meneghesso, E. Zanoni, D. Buttari, S. Heikman, S. Keller, and U. K. Mishra, *Electron. Lett.*, **39**, 625 (2003).
3. J. P. Ibbetson, P. T. Fini, K. D. Ness, S. P. DenBaars, J. S. Speck, and U. K. Mishra, *Appl. Phys. Lett.*, **77**, 250 (2000).
4. M. Miyoshi, Y. Kuraoka, M. Tanaka, and T. Egawa, *Appl. Phys. Express*, **1**, 081102 (2008).
5. J. H. You, J.-Q. Lu, and H. T. Johnson, *J. Appl. Phys.*, **99**, 033706 (2006).
6. N. G. Weimann, L. F. Eastman, D. Doppalapudi, H. M. Ng, and T. D. Moustakas, *J. Appl. Phys.*, **83**, 3656 (1998).
7. C. Skierbiszewski, K. Dybko, W. Knap, M. Siekacz, W. Krupczynski, G. Nowak, M. Bockowski, J. Lusakowski, Z. R. Wasilewski, D. Maude, et al., *Appl. Phys. Lett.*, **86**, 102106 (2005).
8. K. H. Lee, S. J. Chang, P. C. Chang, Y. C. Wang, and C. H. Kuo, *J. Electrochem. Soc.*, **155**, H716 (2008).
9. J. W. P. Hsu, M. J. Manfra, D. V. Lang, S. Richter, S. N. G. Chu, A. M. Sergent, R. N. Kleiman, L. N. Pfeiffer, and R. J. Molnar, *Appl. Phys. Lett.*, **78**, 1685 (2001).
10. J. Ebert, L. Ivanova, S. Borisova, H. Eisele, A. Laubsch, and M. Dahne, *Appl. Phys. Lett.*, **94**, 062104 (2009).
11. J. W. P. Hsu, M. J. Manfra, S. N. G. Chu, C. H. Chen, L. N. Pfeiffer, and R. J. Molnar, *Appl. Phys. Lett.*, **78**, 3980 (2001).
12. J. Elsner, R. Jones, P. K. Sitch, V. D. Porezag, M. Elstner, T. Frauenheim, M. I. Heggie, S. Oberg, and P. R. Briddon, *Phys. Rev. Lett.*, **79**, 3672 (1997).
13. D. Cherns and M. Hawkrige, *J. Mater. Sci.*, **41**, 2685 (2006).
14. Y.-Y. Wong, E. Y. Chang, T.-H. Yang, J.-R. Chang, Y.-C. Chen, J.-T. Ku, C.-T. Lee, and C.-W. Chang, *J. Cryst. Growth*, **311**, 1487 (2009).
15. C. D. Lee, A. Sagar, R. M. Feenstra, C. K. Inoki, T. S. Kuan, W. L. Sarney, and L. Salamanca-Riba, *Appl. Phys. Lett.*, **79**, 3428 (2001).
16. P. Waltereit, C. Poblenz, S. Rajan, F. Wu, U. K. Mishra, and J. S. Speck, *Jpn. J. Appl. Phys.*, Part 2, **43**, L1520 (2004).
17. S. Vézian, F. Natali, F. Semond, and J. Massies, *Phys. Rev. B*, **69**, 125329 (2004).
18. J. C. Zhang, D. G. Zhao, J. F. Wang, Y. T. Wang, J. Chen, J. P. Liu, and H. Yang, *J. Cryst. Growth*, **268**, 24 (2004).
19. B. Heying, X. H. Wu, S. Keller, Y. Li, D. Kapolnek, B. P. Keller, S. P. DenBaars, and J. S. Speck, *Appl. Phys. Lett.*, **68**, 643 (1996).
20. P. Gay, P. B. Hirsch, and A. Kelly, *Acta Metall.*, **1**, 315 (1953).
21. D. Jena, in *Polarization Effects in Semiconductors, from Ab Initio Theory to Device Applications*, C. Wood and D. Jena, Editors, p. 161, Springer, New York (2007).
22. W. S. Tan, P. A. Houston, M. J. Uren, R. S. Balmer, J. L. Gasper, and T. Martin, in *2nd EMRS DTC Technical Conference*, United Kingdom Ministry of Defense, p. A27 (2005).
23. E. J. Miller, E. T. Yu, P. Waltereit, and J. S. Speck, *Appl. Phys. Lett.*, **84**, 535 (2004).